Lawrence Berkeley National Laboratory
Recent Work

Title
SOLUTE-SOLUTE INTERACTIONS OF MATRIX ISOLATED Cu, Ag, AND Au ATOMS

Permalink
https://escholarship.org/uc/item/8cc8h9gb

Authors
Brewer, Leo
King, Baldwin

Publication Date
1970-06-01

SOLUTE-SOLUTE INTERACTIONS OF
MATRIX ISOLATED Cu, Ag, AND Au ATOMS

Leo Brewer and Baldwin King

June 1970

LAWRENCE RADIATION LABORATORY
UNIVERSITY of CALIFORNIA BERKELEY

DISCLAIMER

Solute-Solute Interactions of Matrix Isolated Cu, Ag, and Au Atoms

Leo Brewer and Baldwin King [†]

Inorganic Materials Research Division of the
Lawrence Radiation Laboratory,
and the Department of Chemistry of
the University of California,
Berkeley, California 94720

Abstract

We examined the matrix spectra of Cu, Ag, and Au separately in

matrices of Ar, Kr, Xe, and SF_6 and compared them with the spectra of

the pairs Ag and Au and Cu and Au in Kr. We observed that the spectra

of the metal atoms were identical whether deposited separately or in

pairs and we can exclude solute-solute interaction as a source of the

shifts, splitting and broadening of atomic lines compared to the gaseous

spectra. Similar results were obtained for combinations of Cu, Au, and

Hg. We also studied the spectrum of Au atoms in mixtures of Kr and SF_6.

[†] Present address: Photo Products Division, Du Pont Corporation, Parlin, N. J.

Introduction

Matrix isolation of high temperature molecules in inert matrices at low temperatures offers the possibility of simplification of molecular spectra by reduction of electronic, vibrational, and rotational excitation. The method has been found useful in many laboratories for the study of high temperature molecules.[1] However matrix spectra suffer from unanticipated complexities in that even the strong features are often rather broad, considerably shifted from the gas phase positions, and show splitting or extra features that confuse the interpretation of the spectra. A study of atomic spectra in inert matrices was initiated[2,3] in the hope that the simpler atomic spectra would make it easier to characterize the origin of the matrix spectral complexities.

Two general explanations of the extra features of matrix spectra have been offered. The first[1,4-10] ascribes the extra eatures to interactions between the solute and the surrounding matrix molecules either as a result of multiple sites in the matrix or through removal of orbital degeneracy. The second[1,10,11,22] ascribes the extra features to interactions between pairs of solute species. Nearest-neighbor pair interactions can be usually excluded from consideration by considering only features which persist even to high dilutions; thus long range interactions between non-nearest-neighbor pairs must be invoked.

We have devised a test of the assumption of long range interactions as the source of extra spectral features of solute atoms. First we isolated Cu, Ag, and Au atoms separately in Ar, Kr, Xe, and SF_6. If the principal spectral features depended to any appreciable extent upon long range interactions between solute pairs, the replacement of

some solute neighbors by atoms of another metal should produce a

change in the spectrum. The pairs Ag and Au and Cu and Au were

codeposited in krypton. We found the principal spectral features to

be indistinguishable within experimental error from the spectra obtained

for each of the atoms deposited separately, and solute-solute interactions

can be excluded as a source of the major features of the Kr matrix spectra

of Cu, Ag, and Au.

Experimental

Atomic beams of Cu, Ag, and Au were generated from spectroscopic

grade graphite Knudsen cells, heated either by resistance heating or

electron bombardment. The graphite resistance furnace described earlier[2,3,12]

was used for single element deposition or for vaporization of alloys of

two elements, but it was more satisfactory to use a double Knudsen cell

from which the two metals could be simultaneously and independently

vaporized using electron bombardment.

The double graphite cell was screwed onto the threaded end of a

6 mm diameter tantalum rod which was fused to a short piece of nickel

tubing and this in turn was hard-soldered to an electrically-insulated

Kovar-porcelain feedthrough. Two tungsten heating filaments,

30 mm x 0.75 mm x 0.025 mm, were spot-welded to three tungsten support

rods, 1 mm in diameter, which were first capped with tantalum foil.

Two of the three rods served as current leads while the third was

grounded. All three exited through a brass flange by means of Kovar-

porcelain feedthroughs. The Knudsen cells and the surrounding tungsten

filaments were enclosed by three concentric cylindrical tantalum radiation

shields. A 6.4 mm diameter aperture served to collimate the atomic beam.

The filaments were operated at typically 7 v and 8 a. By radiation

heating alone, the Knudsen cell reached a temperature of about 1100°K.

A positive potential of 700 volts applied to the Knudsen cell with an

electronic bombardment current of 150 mA produced a temperature of

about 1350°K which could be maintained to within ten degrees without

any special controls on the filament current. The Knudsen cells were

heated to attain metal vapor pressures of 2×10^{-4} to 10^{-3} torr.

Typical temperatures for Ag, Cu, and Au were 1150, 1350, and 1400°K,

respectively. The concentrations in the matrices were calculated from

the flow rate of matrix gas and the calculated flow of the atoms from

the Knudsen cell assuming complete condensation upon the target.

The metal cryostat using liquid hydrogen as refrigerant, the

spectroscopic equipment, and the operational procedures were described

earlier[2,13,14]. The background continuum for the ultraviolet was provided

by a 150 watt xenon-mercury lamp operating at 8 amp. A 1 kilowatt hydrogen

discharge lamp was also used, mainly in the study of gold below 250 nm.

A low pressure mercury "germicidal" lamp served as the reference source.

Slit widths were normally 60 μm with exposure times ranging from 1/10 second

to 5 minutes. Kodak 103a-O plates were used down to 245 and Kodak Shortwave

Radiation (SWR) plates were used below 245 nm. Transmission spectra were

taken through the matrix and the sapphire target, but in a few experiments

with silver the matrix film was deposited on highly polished aluminum and

specular reflectance spectra were taken with an incident beam angle of 45°.

We obtained identical spectra by both methods.

Results for Single Metal Deposition

Meyer[1] has reviewed previous work on the matrix isolation of Cu, Ag, and Au. Three strong features are observed usually within 2000 cm^{-1} of the position of the $^2P_{1/2,\ 3/2} \leftarrow ^2S_{1/2}$ gaseous transition with one or more weaker bands often reported. For Au, the 3829 cm^{-1} separation of the $^2P_{1/2}$ and $^2P_{3/2}$ multiplet makes the assignment of the three strong features clear. The band to the red is assigned to the $^2P_{1/2} \leftarrow ^2S_{1/2}$ transition with the normally degenerate sublevels of the $^2P_{3/2}$ level being split by 500 to 600 cm^{-1} in Kr and Xe. The comparisons of the Cu and Ag matrix spectra with the Au spectra then provide for similar assignments of the red member of each triplet to $^2P_{1/2} \leftarrow ^2S_{1/2}$ and of the two violet members to $^2P_{3/2} \leftarrow ^2S_{1/2}$. The fluorescent studies of Meyer and Currie[15] provide a direct confirmation of these assignments for Cu.

The present work on Cu, Ag, and Au, isolated separately, is in essential agreement with the earlier studies.[1,3,15,16,20] For copper the half-widths at 20° K of the three strong bands decreased from 450 cm^{-1} in Kr to 300 cm^{-1} in Xe. For silver in Ar, the singlet had a half-width of the order of 350 cm^{-1} while the other two bands were not completely resolved and had half-widths of the order of 400 to 500 cm^{-1}. In Kr, the half widths were 250 cm^{-1} and in Xe, 200 cm^{-1}. In contrast to the increase in sharpness for Cu and Ag bands as the matrix atom became heavier, Au in Kr had a half-width of 100 cm^{-1} increasing to 450 cm^{-1} in Xe. Cu and Ag have been isolated in SF_6 matrices yielding very broad spectra.[17] However gold in SF_6 was quite unique in yielding bands with

half-widths of only 75 cm^{-1}, sharper than observed in any rare gas

matrices. The spectrum in SF$_6$ was also unique in that the $^2P_{3/2} \leftarrow {}^2S_{1/2}$

transition did not separate into two clear features as observed in the

rare gas matrices for Cu, Ag, and Au. Figure 1 shows the spectrum of

Au in SF$_6$ and Kr. For those systems with broad bands with half-widths

of 350 cm^{-1} or more, very long deposition times with relatively high

vapor pressure sources were required to obtain even moderately strong

bands. On the other hand, we could obtain very strong absorption in

30 minutes for Ag in Xe with a 1140°K Knudsen cell source or for Au in

Kr with a 1420°K source.

We studied the effect of the target temperature upon the spectra

by removing the liquid hydrogen from the dewar. When the target had

warmed up to a desired temperature as monitored by a germanium thermistor,

the spectrum was taken and the target quickly cooled to 20°K by reintroduction

of the liquid hydrogen. The spectrum was then taken at 20°K and the

warmup procedure repeated to a higher temperture. This was continued

until the absorption spectrum had disappeared. Little change was seen

upon warming when the band half-widths were 400 cm^{-1} or more, but for

sharper bands, the half-width increased upon warmup and the peaks shifted,

mainly to the red. Upon recooling to 20°K, the spectra returned

reversibly to its original condition. All of the spectra with sharp features

showed large temperature dependencies of the type shown in Fig. 4 of

reference 3.

Tables I, II, and III give the observed peak positions, assignments,

and shifts from the gaseous atomic line positions for Cu, Ag, and Au,

respectively, for typical experiments. The character of the bands are

indicated by (s), strong; (m), medium; (w), weak. We give no assignments

for weak bands which appeared only at high concentrations. They might

be due to dimers, but we saw no bands at wavelengths where bands are
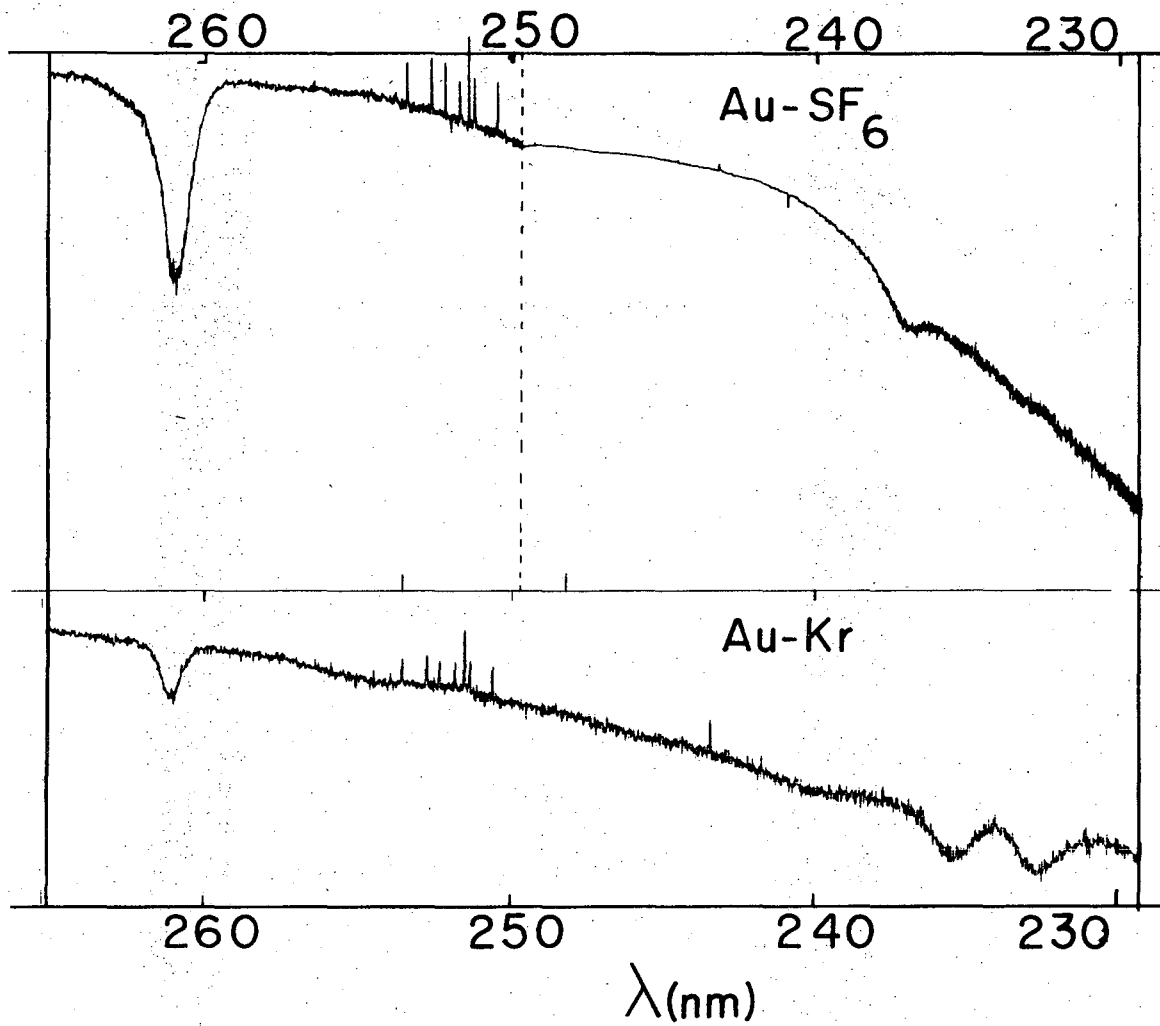
Figure 1. Absorption spectra of matrix-isolated gold.

XBL 6810-6043

Table I.

Absorption Spectra of Matrix-Isolated Copper at $20°$ K.

Matrix	λ (nm)	ν (cm^{-1})	Assignment	Shift from Gas cm^{-1}
Krypton 0.4 at %	325.5 ± 0.5	30 700 (w)	?	
	314.8 ± 0.5	31 770 (m)	$^2P_{1/2} \leftarrow {}^2S_{1/2}$	+ 1230
	311.1 ± 0.5	32 140 (m) ⎫	$^2P_{3/2} \leftarrow {}^2S_{1/2}$	+ 1360
	307.5 ± 0.5	32 520 (m) ⎭		+ 1740
Xenon 2 at %	326.3 ± 0.5	30 650 (s)	$^2P_{1/2} \leftarrow {}^2S_{1/2}$	+ 110
	323.7 ± 0.5	30 890 (s) ⎫	$^2P_{3/2} \leftarrow {}^2S_{1/2}$	+ 110
	320.1 ± 0.5	31 240 (s) ⎭		+ 460

Weak features at 283.1, 273.5, 266.4, 248.5, and 247.0 nm.

Table II.

Absorption Spectra of Matrix-Isolated Silver at 20°K.

Matrix	λ(nm)	ν(cm^{-1})	Assignment	Shift from Gas cm^{-1}
Argon 0.25 at %	330.9 ± 1.0	30 200 (w)	?	
	315.0 ± 0.5	31 750 (s)	$^2P_{1/2} \longleftarrow {}^2S_{1/2}$	+ 2190
	304.1 ± 0.5	32 880 (m)	$^2P_{3/2} \longleftarrow {}^2S_{1/2}$	+ 2410
	298.6 ± 0.5	33 490 (m)		+ 3020
Krypton 0.7 at %	322.7 ± 0.5	30 990 (s)	$^2P_{1/2} \longleftarrow {}^2S_{1/2}$	+ 1440
	313.6 ± 0.5	31 890 (s)	$^2P_{3/2} \longleftarrow {}^2S_{1/2}$	+ 1420
	309.4 ± 0.5	32 320 (s)		+ 1850
Xenon 0.5 at %	334.6 ± 0.3	29 890 (s)	$^2P_{1/2} \longleftarrow {}^2S_{1/2}$	+ 330
	327.3 ± 0.3	30 550 (s)	$^2P_{3/2} \longleftarrow {}^2S_{1/2}$	+ 80
	325.7 ± 0.3	30 700 (m)	$^2D_{3/2} \longleftarrow {}^2S_{1/2}$	- 4010
	322.6 ± 0.3	31 000 (s)	$^2P_{3/2} \longleftarrow {}^2S_{1/2}$	+ 530

Table III.

Absorption Spectra of Matrix-Isolated Gold at 20°K

Matrix	λ(nm)	ν(cm^{-1})	Assignment	Shift from Gas cm^{-1}
SF$_6$ 0.7 at %	298.1 ± 0.5	33 550 (w)	?	
	261.0 ± 0.2	38 310 (s)	$^2P_{1/2} \leftarrow ^2S_{1/2}$	+ 950
	237.8 ± 0.2	42 050 (s)	$^2P_{3/2} \leftarrow ^2S_{1/2}$	+ 880
Krypton 0.3 at %	335.6 ± 0.5	29 800 (w)	?	
	271.1 ± 0.5	36 900 (w)	?	
	261.1 ± 0.2	38 300 (s)	$^2P_{1/2} \leftarrow ^2S_{1/2}$	+ 940
	239.9 ± 0.2	41 680 (w)	?	
	235.3 ± 0.4	42 500 (s) }	$^2P_{3/2} \leftarrow ^2S_{1/2}$	+ 1330
	232.5 ± 0.4	43 010 (s) }		+ 1840
Xenon 0.33 at %	271.3 ± 1.0	36 860 (w)	$^2P_{1/2} \leftarrow ^2S_{1/2}$	− 500
	247.8 ± 1.0	40 350 (m) }	$^2P_{3/2} \leftarrow ^2S_{1/2}$	− 820
	244.1 ± 1.0	40 970 (m) }		− 200

reported[18,19] in the gaseous spectra of Cu_2, Ag_2, or Au_2. Even though some of these gaseous spectral bands are seen in absorption in the King furnace and must arise from low-lying states, there is no assurance that these bands involve the ground state and would be observed in the low temperature matrix. Meyer and Currie[15] have observed Cu_2 progressions in Kr and Xe. The weak features at 283, 274, and 266 nm listed in Table I for Cu in Xe correspond to features identified as Cu_2 bands by Meyer and Currie. In the study of the spectrum of Cu sputtered in xenon, Shirk and Bass[20] had assigned the 247 nm feature to the forbidden $^4P \leftarrow {}^2S$ transition and had attributed the 248.5 and 283 nm features to impurities. Meyer and Currie[15] suggest that the 248.5 nm feature could also be a portion of the $^4P \leftarrow {}^2S$ transition. Table II lists only three features for 0.7 at % Ag in Kr as the fourth band reported earlier[3] appears only at much higher silver concentrations than those used in this study. In addition to the strong absorptions from the ground state to the $^2P_{1/2}$ and $^2P_{3/2}$ states, one band observed at 325.7 nm for silver in Xe was unique in that it was reproducible at all concentrations of silver in contrast to weak bands of other systems that appear only at high concentrations. This band is clearly not due to an impurity. We have made somewhat tenuous assignment to the $^2D_{3/2} \leftarrow {}^2S_{1/2}$ transition which is forbidden in the gas but which would be expected to be greatly strengthened by mixing of the ^2P and ^2D states due to interaction with the heavy xenon. However, the red shift of 4010 cm^{-1} seems too large although we could assume that the mixing of states might produce an unusually large shift. For Cu and Au where the $^2D_{3/2}$ state is about 20,000 cm^{-1} below the $^2P_{3/2}$ state, we see no similar bands in xenon.

We carried out very detailed studies of silver in Kr to determine

the effect of various variables upon matrix spectra. The concentration

was varied from 1 to 0.025 atomic percent by keeping the temperature

of the Knudsen cell constant and changing the flow rate of Kr. Also a

number of matrices with the same concentration were prepared using

different deposition times, Knudsen cell temperatures, and Kr flow rates.

Over the range of variation studied, the spectra were almost identical.

The half-widths of the bands were of the order of 250 cm^{-1} and the

occasional slight variations in half-width depended more upon the optical

thickness of the samples rather than the concentration of silver. The

warm-up procedure described above was used to determine if annealing

of the matrix might change the spectrum, but the spectra returned to their

original condition upon recooling. We attempted to synthesize the dimer

by warming the Kr matrix. The band widths increased and the peaks shifted,

but no new features appeared. The silver atomic spectrum remained reasonably

strong even after warmup to about 50°K. These results are similar to

those for mercury[12] but contrast with the observation for the alkali metals[8,10]

at 4°K where two sets of triplets are often observed with one set disappearing

upon warmup and with formation of dimers upon warmup to yet higher

temperatures at which diffusion can take place. The apparent lack

of annealing effects upon warmup of silver deposited in krypton at 20°K

may be due to prior annealing by the furnace radiation during deposition.

For a furnace temperature of 1336°K the radiant heat input from the
                                                              5 cm away
furnace was 4 x 10^{-4} cal sec^{-1} mm^{-2} at the center of the sapphire plate /

or several orders of magnitude greater than the heat of condensation of

the matrix and metal atoms at a deposition rate of 0.5 millimoles of gas

per hour. We believe that all of our observed spectra correspond to

fully annealed samples. This requires that there be enough mobility

during deposition to allow the silver atoms and the surrounding

krypton atoms to attain the most stable configuration at a given

lattice site. Since we found no evidence for silver polymers nor

any differences in the spectra of silver in krypton for concentrations

from 0.025 to above 1 atomic percent, subsequent experiments were mostly

restricted to the range from 0.2 to 0.5 atomic percent Ag.

## Results for Mixed Metal Deposition

We inadvertently admitted Hg vapor several times when Cu was deposited in

Xe and Au in Kr with no apparent effect upon the Cu, Au, or Hg spectra.

Similar results have been observed[21] for Mg together with Cd or Ca.

As it might be argued that long range interactions would not be expected

for atoms with ^1S ground states, we felt that a mixture of atoms with

unpaired electrons would provide a better test of long range interactions.

Ag and Au were vaporized simultaneously in electron bombardment heated

Knudsen cells and codeposited with Kr at 20°K. Gold and silver spectra

of comparable strength were obtained with twice as much silver as gold,

but Ag/Au was varied from 2 to 1/2. The total concentration of metallic

atoms was varied from 0.2 to 0.7 atomic percent. Table IV lists the

measured peak wavelengths of an 0.7 at % matrix for comparison with the

values in Tables II and III for the elements deposited separated.

The spectra of the pure metal (a,b) and the mixed metals (a', b')

in krypton are compared in Fig. 2 for a matrix with a total metal content

Table IV.

Absorption spectra for silver and gold codeposited
in krypton at 20°K, 0.7 at % total metal content.

λ (nm)	ν (cm^{-1})	Assignment
322.8 ± 0.5	30 980 (s)	$^2P_{1/2} \leftarrow {}^2S_{1/2}$ Ag
313.8 ± 0.5	31 870 (s) ⎫	
309.5 ± 0.5	32 310 (s) ⎭	$^2P_{3/2} \leftarrow {}^2S_{1/2}$ Ag
261.1 ± 0.2	38 300 (s)	$^2P_{1/2} \leftarrow {}^2S_{1/2}$ Au
239.5 ± 0.2	41 750 (w)	Au ?
235.3 ± 0.4	42 500 (s) ⎫	
232.7 ± 0.4	42 970 (s) ⎭	$^2P_{3/2} \leftarrow {}^2S_{1/2}$ Au
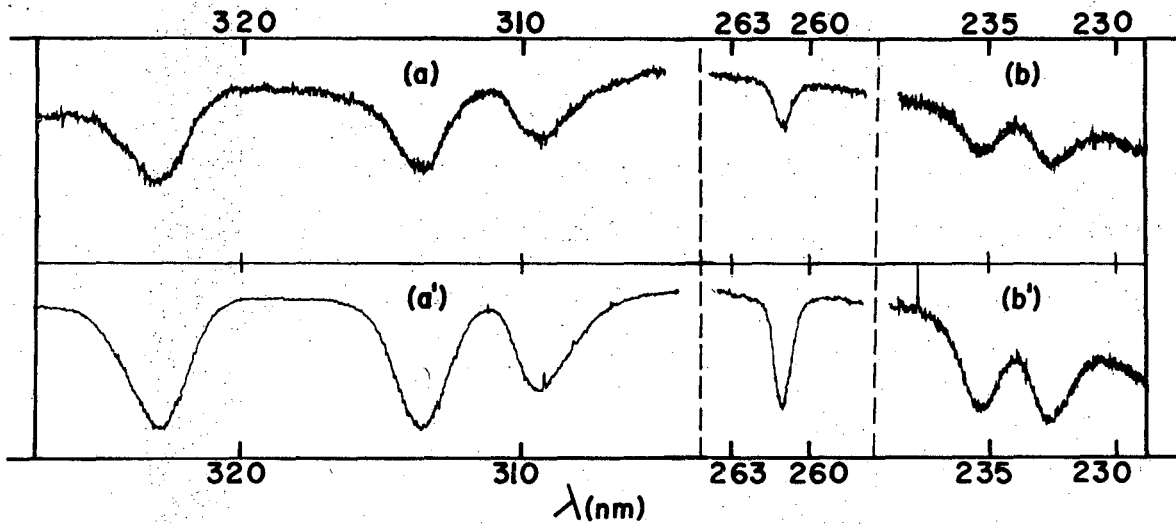
Figure 2. Absorption spectra of silver and gold isolated in krypton (a,b) separately; (a',b') simultaneously. Concentration of silver is 0.5 at % and of gold is 0.2 at %.

of 0.7 at % (0.5 at % Ag and 0.2 at % Au). Only the shapes and

positions are comparable. The relative intensities have no significance

since the photographic plates were not calibrated and different densitometer

settings were used for tracing different sections of the spectrum.

Cu and Au were vaporized simultaneously from an alloy with a

molefraction of copper of 0.28 which was chosen to provide comparable

vapor pressures of around 4×10^{-5} torr of Cu and Au at 1350°K. Mercury

atoms were also present as a contaminant. The gold absorption bands were

much more intense and narrower than those of copper, as for matrices

with single metal deposition. Table V lists, for comparison with the

values in Tables I and III for pure metal matrices, peak wavelengths

for a matrix with the Cu/Au ratio about two and the total of Au and

Cu around 0.1 at % in Kr.

The strong spectral features of the mixed metal matrices corresponded

exactly to those of the pure metal matrices plus the addition of the

strong Hg line at 248.7 nm. Tables I and III indicate that weak impurity

or polymer features were seen to lower concentrations for Cu and Au in

Kr than for Ag. However most of the weak features listed in Table V

do not correspond to those in Tables I and III. This might be taken

to indicate that these weak features are due to mixed polymers

of Hg, Cu and Au. However, additional experiments at higher metal concentrations

without Hg contamination would be necessary for any clear identification.

These observations are conclusive evidence that the observation

of three strong bands in the matrix compared to two lines for the gas

is not due to solute-solute interaction. If they were, the mixed atom

interactions would surely be different than the like atom interactions

and substantial shifts would have been observed. Let us examine the

statistics of the silver-krypton system with 0.2 atomic percent silver.

Table V.

Absorption Spectra for Gold and Copper
(Plus Mercury Contaminant) Codeposited in Krypton at 20°K.

| λ (nm)	ν (cm^{-1})	Assignment
314.2 ± 0.5	31 830 (m)	$^2P_{1/2} \leftarrow\; ^2S_{1/2}$ Cu
311.1 ± 0.5	32 140 (m) ⎫	
307.3 ± 0.5	32 540 (m) ⎭	$^2P_{3/2} \leftarrow\; ^2S_{1/2}$ Cu
271.2	36 900 (w)	Au ?
260.9 ± 0.2	38 330 (s)	$^2P_{1/2} \leftarrow\; ^2S_{1/2}$ Au
248.7	40 210 (v.s.)	$^1P \leftarrow\; ^1S$ Hg
239.2	41 800 (w)	Au ?
235.5 ± 0.5	42 480 (m) ⎫	
232.6 ± 0.5	42 990 (m) ⎭	$^2P_{3/2} \leftarrow\; ^2S_{1/2}$ Au

Also weak broad features at 334.4, 325.5, 321.6, 292.5, and 283.9 nm.

For simplicity the metal atom is assumed to be present in a substitutional
site having 10 nearest neighbors and 20 next-nearest neighbors. An
isolated silver atom is designated as Ag Kr, a silver atom with another
silver atom as a nearest neighbor as Ag Ag, and one having a silver
atom as next nearest neighbor as Ag Kr Ag. The ratio of probabilities
of these three groups is 50:1:2 or for 56 atoms arriving in the lattice,
50 will be present as Ag Kr, 2 as Ag Ag, and 4 as Ag Kr Ag. For Au-Kr
of the same concentration, the same values apply, namely, 89.5, 3.5, and 7%
for the respective sites. If silver and gold are codeposited in equal
amounts at concentrations of 0.1 atomic percent each or a total metal
concentration of 0.2 atomic percent, similar arguments suggest that
again 89.5% of the total number of atoms will be isolated as Ag Kr and
Au Kr in equal amounts; 3.5% will be present as Au Au, Ag Ag, and Au Ag
pairs, the number of each pair being equal; and 7% as Au Kr Au, Ag Kr Ag,
and Au Kr Ag again evenly distributed. The above calculations assume a
uniform distribution. Any tendency for aggregate formation due to diffusion
during condensation and annealing would increase contributions from solute-
solute interactions. If any of the spectral features are due to nearest
neighbor or next-nearest neighbor or even longer range solute-solute
interactions in the pure metal experiments, spectral features of comparable
strength should be observed in the mixed metal experiments due to interactions
between the unlike atoms. The fact that these effects were not observed
for Ag/Au = 2, 1, and 1/2 and for total metal concentrations of 0.2,
0.3, and 0.7 atomic percent demonstrates that none of the three main bands
in the pure metal matrix spectrum are due to solute-solute interactions.
Under the conditions investigated, the atoms responsible for the main spectral
features in the pure or mixed experiments are efficiently shielded from
the effects of other trapped atoms by the atoms of rare gas, and the

splitting of the gaseous doublet into a triplet, the broadening of the
lines, and the shifts from the gaseous positions of up to 3000 cm^{-1}
must be due to interactions between the metal atom and the surrounding
rare gas atoms.

Results for Mixed Matrix Deposition

The previous experiments have demonstrated that the distinctive
features of the matrix spectra are due to interactions between the
solute atom and the surrounding matrix atoms; we examined the effect
of changing the asymmetry of the matrix environment by trapping gold
atoms at 20°K in various mixtures of krypton and sulfur hexafluroide.
Krypton and sulfur hexafluoride gases were mixed and equilibrated for
at least eighteen hours to insure uniformity. Gold temperatures of
1350-1375°K were used and concentrations were varied between 0.14
to 0.25 atomic percent. Figure 3 shows the spectra and Table VI lists
measurements for band peaks. The long wavelength peak $(^2P_{1/2} \leftarrow {}^2S_{1/2})$
has almost exactly the same position in pure Kr or pure SF$_6$, but as
the proportion of Kr in SF$_6$ increased, this peak shifted to the red
by 260 cm^{-1}. This feature which is very sharp in the pure matrices
almost doubled in width in the mixtures. The short wavelength transition
$(^2P_{3/2} \leftarrow {}^2S_{1/2})$ is shifted more from the gas value in pure Kr and is
split by 510 cm^{-1} compared to no detectable splitting in SF$_6$. As Kr is
added to SF$_6$ two features develop, both considerably broader than in the
pure matrices. One of these remains close to the pure SF$_6$ position with
a shift first to the red by 110 cm^{-1} and then a comparable shift to
the other side of the pure SF$_6$ position. The other feature gradually
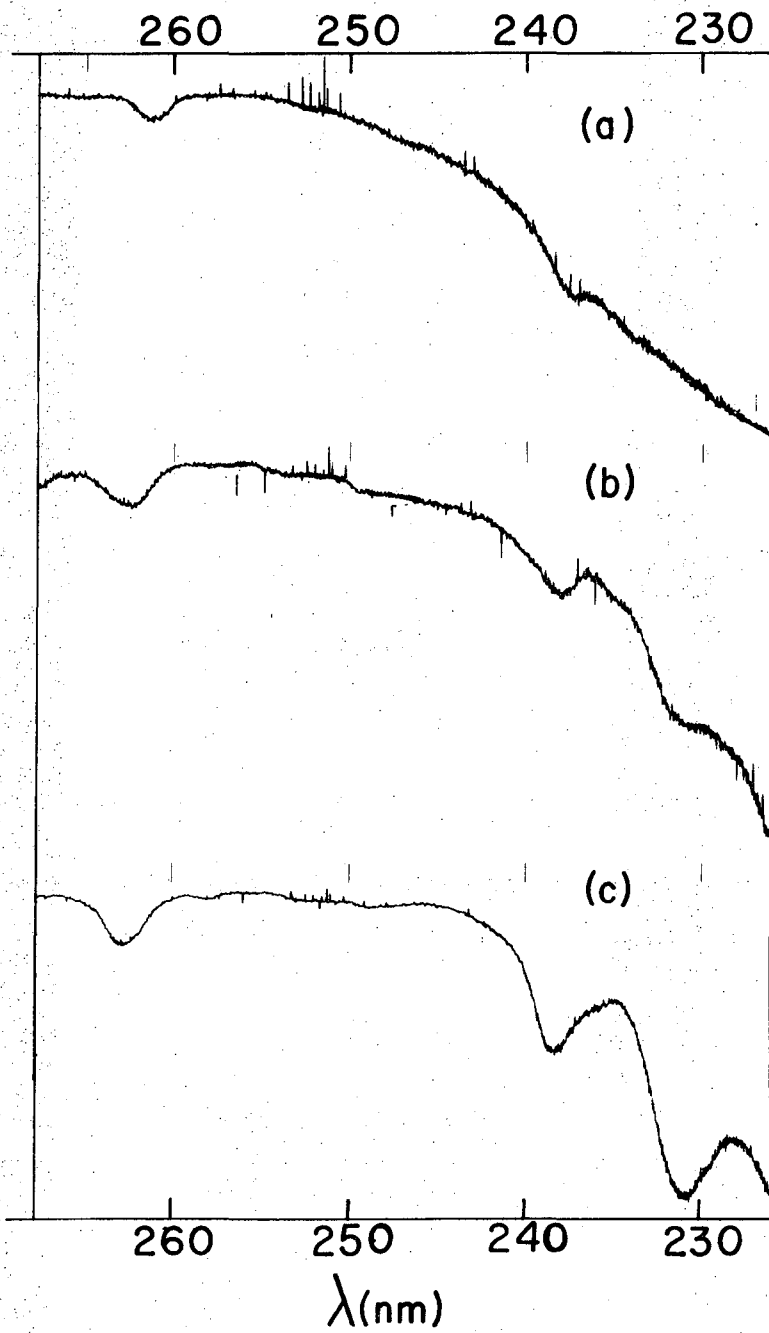
XBL 6810-6045

Figure 3. Absorption spectra of gold trapped in solid SF_6-Kr mixtures (a) 17 mole-% Kr, (b) 50 mole-% Kr, and (c) 83 mole-% Kr.

Table VI.

Absorption Spectra of Gold Isolated

in Kr-SF$_6$ Mixtures at 20°K.

Atomic %	λ (nm)	ν (cm^{-1})	Δ(cm^{-1}) cf. SF$_6$	Δ(cm^{-1}) cf. Kr
7% Kr	261.1	38 300	- 15	0
0.14% Au	237.7	42 070	+ 20	- 30
	233.7	42 790		-220
17% Kr	261.1	38 300	- 15	0
0.2 % Au	237.2	42 160	+ 10	-340
	232.8	42 950		- 60
50% Kr	262.5	38 095	-220	-200
0.17% Au	238.2	41 980	- 70	-520
	230.8±0.5	43 330		+320
75% Kr	262.8	38 050	-260	-250
0.3% Au	238.8	41 880	-175	-620
	230.5	43 380		+370
83% Kr	262.8	38 050	-260	-250
0.25% Au	238.5	41 930	-120	-570
	231.0	43 290		+280

intensifies as Kr is added and remains close to the position of the
shortest wavelength feature in pure Kr with a maximum shift of 370 cm^{-1}
in 75 atomic percent Kr. One might be tempted to describe the spectrum
in terms of segregation into SF_6 rich sites and Kr rich sites, but even
in 83% Kr, there are no signs of the feature found at 235.3 nm in pure
Kr. One would have to ascribe the feature found between 238 and 239 nm
to a blend of the band found at 237.8 nm in SF_6 and at 235.3 nm in
Kr with red shifts up to 600 cm^{-1} for the Kr feature. If this
interpretation is made, the $^2P_{3/2}$ level, which is split by 510 cm^{-1}
in pure Kr, increases its splitting to 1000 cm^{-1} in 75% Kr and then
decreases to 210 cm^{-1} in 7% Kr with the short wavelength component
becoming weaker and weaker with only a broad feature observable in
pure SF_6.

Summary

The experiments with mixed metal matrices containing Cu, Ag, Au,
and Hg in Kr demonstrate that the shifts from the gaseous spectral line
positions, the splitting of the gaseous doublets into triplets, and the
increased line widths cannot be attributed to solute-solute interaction
and must be due to interaction between the metallic atoms and the
krypton atoms.

The half-width variation from 450 cm^{-1} for Cu to 250 cm^{-1} for Ag and
100 cm^{-1} for Au in Kr might be attributed to different conditions of
preparation of each matrix such as the effect of different intensities
of radiation from the furnaces. However, the persistence of these line-width
differences when pairs of metals were deposited together demonstrates
that there are real differences in the interaction with the krypton.

It is possible that the variation is due to the smaller atoms occupying a greater variety of lattice sites, e.g. substitutional and interstitial sites as well as different coordination numbers for each type of site. If this is so, the distribution of sites occupied by Cu, Ag, and Au atoms is not changed by warming the matrix to as high as 50° K as the substantial spectral changes with temperature were reversible upon cooling.

The splitting of the $^2P_{3/2}$ level in the rare gas matrices has been ascribed to removal of degeneracy by an asymmetric environment.[5,6] The mixed Kr-SF$_6$ matrix results could be interpreted in terms of an increase in splitting from 510 cm^{-1} for Au in pure Kr to 1000 cm^{-1} in a mixture of 75% Kr and 25% SF$_6$. However the weakening of the second component of the pair upon addition of more SF$_6$ is difficult to explain.

References

1. Beat Meyer, Science, 168, 783   (1970) and Chapter 9 in
    "Low Temperature Spectroscopy; Optical Properties of Molecules in
    Matrices, Mixed Crystals and Glasses, Elsevier, to be published 1970.

2. L. Brewer, B. Meyer, and G. D. Brabson, J. Chem. Phys. 43, 3973-80 (1965).

3. L. Brewer, B. King,   J. L. Wang, B. Meyer, and G. F. Moore,
    J. Chem. Phys. 49, 5209-13 (1968). Figure 4 of this paper is
    confusing as it was printed upside down.

4. M. McCarthy, Jr. and G. W. Robinson, Mol. Phys. 2, 415 (1959).

5. O. Schnepp, J. Phys. Chem. Solids 17, 188 (1961).

6. M. Brith and O. Schnepp, J. Chem. Phys. 39, 2714 (1963).

7. W. Weyhmann and F. M. Pipkin, Phys. Rev. 137, A490 (1965).

8. B. Meyer, J. Chem. Phys. 43, 2986 (1965).

9. W. M. Duley, Proc. Phys. Soc. 88, 1049 (1966).

10. L. Andrews and G. C. Pimentel, J. Chem. Phys. 47, 2905 (1967).

11. R. B. Merrithew, G. V. Marusak, and C. E. Blount, J. Mol. Spectros. 29
    54-65 (1969).

12. G. D. Brabson, Ph. D. Thesis, Univ. of Calif. Berkeley, UCRL-11976 (1965).

13. L. Brewer, G. D. Brabson, and B. Meyer, J. Chem. Phys. 42, 1385-89 (1965).

14. L. Brewer and G. D. Brabson, J. Chem. Phys. 44, 3274-8 (1966).

15. B. Meyer and S. Currie, to be published.

16. A. Morelle, Ph. D. Thesis, University of Washington, 1970.

17. L. Brewer, Chin-An Chang, and B. King, Inorg. Chem. 7, 814 (1970).

18. B. Kleman and S. Lindkvist, Arkiv. för Fysik. 8, 333, 505 (1954);
    9, 385 (1955).

19. C. Shin-Piaw, W. Loong-Seng, and L. Yoke-Seng, Nature, 209, 1300 (1966).

20. J. S. Shirk and A. M. Bass, J. Chem. Phys. $\underline{49}$, 5156 (1968).

21. J. L. Wang, Ph. D. Thesis, Univ. of California, Berkeley,
     UCRL-19093 (1969).

22. M. McCarty, Jr., J. Chem. Phys. $\underline{52}$, 4973(1970).